

Development and Evaluation of Alternative Imaging Methods for fMRI at 7 Tesla

J. Sexton^{1,2}, J. Swisher³, F. Tong³, B. Rogers^{1,2}, J. C. Gatenby^{1,4}, and J. C. Gore^{1,4}

¹Vanderbilt University Institute of Imaging Science, Nashville, TN, United States, ²Biomedical Engineering, Vanderbilt University, Nashville, TN, United States, ³Psychology, Vanderbilt University, Nashville, TN, United States, ⁴Radiology and Radiological Sciences, Vanderbilt University, Nashville, TN, United States

INTRODUCTION

High field (7T) MRI scanners can in principle be used to obtain increases in sensitivity and spatial resolution for fMRI. However, off-resonance effects caused by susceptibility variations become significantly more severe at high field, causing distortions and T²*-related blurring in single-shot methods such as gradient-echo Echo Planar Imaging (EPI), the sequence commonly used for blood oxygen level-dependent (BOLD) fMRI. We have implemented alternative BOLD-sensitive fast imaging sequences for high resolution fMRI which achieve similar temporal resolution for acquiring image volumes, but which are less prone to susceptibility effects. Here we compare 2D-EPI and two multi-shot 3D gradient echo sequences, 3D-FFE and 3D-PRESTO [6-7], in a polar angle retinotopic mapping experiment at four isotropic resolutions (1.12mm³, 1.67mm³, 2mm³, and 3mm³) at 7T.

METHODS

Four healthy, experienced, adult subjects were scanned on a Philips Achieva 7T scanner with 16 channel SENSE receive-only head coil and outer quadrature transmit coil. fMRI data for a polar angle retinotopic mapping experiment were acquired with scan parameters shown in Table 1. All scans were 288 seconds. Subjects were secured with padding and a bite bar and viewed a black and white flashing checkerboard wedge (108 degrees of visual field; alternating at 8 Hz; rotating counterclockwise; period 36 s). Slices were aligned perpendicular to the calcarine sulcus and covered the occipital pole and as many high visual areas as possible. SENSE acceleration factors (R) were chosen to maintain isotropic voxel dimensions, equal slice coverage between sequences, and geometry factors < 2 at each resolution. Data were motion corrected and registered to anatomical images. Sine and Cosine waves with period 36s served as F-contrast regressors. Low frequency fluctuations (period > 128 s) were removed. Phase-encoded retinotopic maps were generated and projected onto inflated cortex models as described previously [1-5]. F-statistics and functional SNR were calculated within V1 using MATLAB (The Mathworks, Inc., Natick, MA).

RESULTS

In all acquisitions we observed robust activation and retinotopic maps in agreement with literature [1-5]. Fig. 1 shows retinotopic maps for a representative subject (color scheme from [2]). Fig. 2 shows median square root F-statistics (a measure of functional SNR [8]). 2D-EPI shows somewhat higher F-statistics than 3D-FFE at 1.12mm³, and 1.67mm³, while 3D-PRESTO shows higher F-values than EPI at 2mm³ and 3mm³ (all significant; p<0.01). Retinotopic maps from our 3D sequences consistently showed less distortion and better specificity to gray matter than EPI.

DISCUSSION

Though EPI has theoretical advantages in efficiency and in obtaining high signal to noise ratios, other technical issues also affect fMRI performance at 7T. By contrast, 3D-FFE and 3D-PRESTO are much less affected by distortion, enjoy theoretical SNR benefits at high resolutions from signal-averaging inherent to 3D imaging, and use 2D-SENSE acceleration to reduce off-resonance effects, shorten scan time, or extend the imaging volume. At 1.12mm³ and 1.67mm³, the slightly higher F-statistics in EPI may well be sacrificed in favor of reduced distortion and other benefits with 3D-FFE. At 2mm³ and 3mm³, 3D-PRESTO achieved significantly higher temporal resolution and F-statistics than EPI for the same imaged volume. Together these findings suggest rich potential for high-resolution 3D imaging sequences in retinotopic mapping and other functional MRI experiments at high field.

REFERENCES

- Engel et al. Nature. 369(6481): 525 (1994).
- Sereno et al. Science. 268(5212): 889-93 (1995).
- DeYoe et al. Proc. Nat. Acad. Sci. U.S.A. 93(6): 2382-2386 (1996).
- Wandell et al. Neuron. 56(2): 366-383 (2007).
- Swisher et al. J. Neurosci. 27(20): 5326-5337 (2007).
- Liu et al. MRM. 30(6): 764-768 (1993).
- Neggens et al. NMR Biomed. 21: 663-676 (2008).
- Warning et al. NeuroImage. 17:1665-1683 (2002).

Table 1: Acquisition Parameters

Resolution (mm ³)		FOV	Slices	TR (ms)	TE (ms)	R	Flip	BW (Fq, Ph) (Hz)
1.12	EPI	144 (FH) 144 (RL)	25	2880	22	2.4	80	1581 (F) 22 (P)
	3D-FFE	28 (AP)		42	22	2.6	20	1571 (F) 63 (P)
1.67	EPI	160 (FH) 160 (RL) 40 (AP)	24	2880	22	2.7	80	2333 (F) 41 (P)
	3D-FFE			31	22	2.6	10	2200 (F) 101 (P)
2	EPI	160 (FH) 160 (RL) 40 (AP)	20	2400	22	2.7	80	2793 (F) 55 (P)
	3D-PRS			19	(6) 26	2.2	10	2662 (F) 114 (P)
3	EPI	192 (FH) 192 (RL) 60 (AP)	20	2400	22	2.6	80	4163 (F) 80 (P)
	3D-PRS			15	(7) 22	1.8	10	4103 (F) 145 (P)

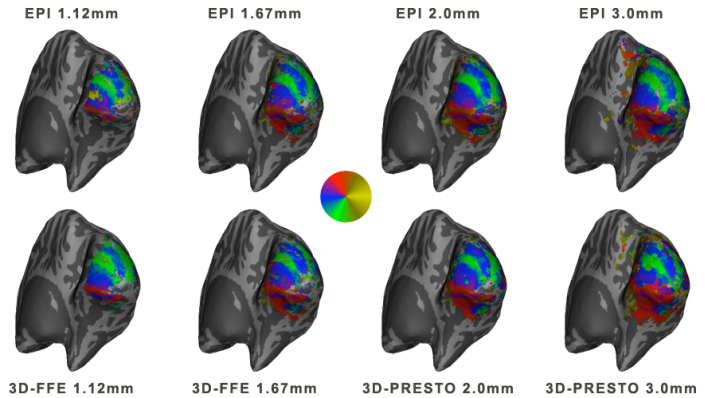


Fig. 1: Retinotopic maps for a representative subject.

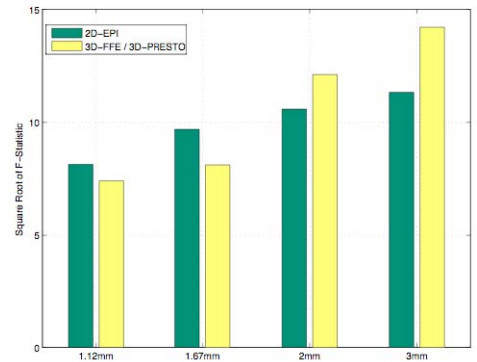


Fig. 2: Median \sqrt{F} -statistics (all subjects).